

Isotope effect in the work function of lithium

Atef A. Sheekhoon, Abdelrahman O. Haridy,* Vitaly V. Kresin*

Department of Physics and Astronomy, University of Southern California,
Los Angeles, 90089-0484, USA

The work functions of ^7Li and ^6Li metals have been measured as a function of temperature, by using photoionization of pure isolated metal nanoparticles in a beam. These data reveal a marked isotope effect in the temperature variation of these work functions. Furthermore, for both isotopes the curvature of this temperature variation is found to be significantly larger than may be ascribed purely to a change in the electron gas density. These findings enhance the characterization of lithium as a quantum material in which the interplay between electronic and ionic degrees of freedom is nontrivial, and call for a microscopic understanding beyond simple models. Additionally, the slope of the work function curves was observed to vanish in the low temperature limit, as had been predicted on the basis of the Third Law of thermodynamics.

*These authors contributed equally to this work.

Introduction.—The interaction between metal conduction electrons and thermal lattice vibrations leads to well-known consequences for electronic kinetic phenomena, such as charge and heat transfer. But interestingly, the presence of vibrational excitations also can affect equilibrium properties of electron spectra. Specifically, here we probe the influence of thermal vibrations on the electronic work function. While the temperature dependence of the work function is not as steep as that of transport coefficients, an accurate measurement of this effect elucidates a distinctive connection between electronic and vibrational degrees of freedom. To spotlight the role of the latter, we focus on the isotope effect by comparing the temperature variations of the work functions of ${}^6\text{Li}$ and ${}^7\text{Li}$.

In addition to having two abundant stable isotopes with sufficiently separated masses, lithium metal possesses other features that make it an interesting subject. The low atomic mass, substantial zero-point motion, and high Debye temperature (320–440 K [1,2]) result in a significant enhancement of quantum effects in its lattice structure and dynamics, giving rise to a range of unusual structural and phase transitions and even superconductivity with an anomalous isotope effect [3,4].

Alongside the low mass, lithium is distinguished by the relatively weak shielding of the atomic nucleus by the 1s core electrons, exposing its conduction electrons to a hard and nonlocal pseudopotential [5–7]. As a result, for example, their optical and thermal effective masses are much more enhanced relative to the free-electron value than in the other alkali metals [8]. Now consider that the work function can be expressed as follows [9,10]:

$$W = -e\Delta\varphi - \bar{\mu} \quad (1)$$

where e is the magnitude of the electron charge, $\bar{\mu}$ is the electron chemical potential inside the metal referred to the electrostatic potential in the interior, and $\Delta\varphi$ is the difference between the latter and the electrostatic potential in the vacuum outside the metal. This implies that for lithium one may anticipate that quantum effects will influence the dependence of W on the temperature and on the isotopic mass: as the material warms up and undergoes thermal expansion, not only does the electron gas density change but so do the band structure, the electron-vibrational coupling strength, the effective mass, the behavior of the surface dipole layer, etc. As will be shown below, simple electrostatic models that can reproduce $W(T)$ for other metals aren't as successful for Li, which underscores the need for a more quantitative theory.

While lithium is a very interesting material to study, many of its physical and chemical properties can be impacted by contamination. Despite sometimes being characterized as “the least reactive” of the alkali group [11], it is the only alkali metal that significantly reacts with nitrogen, and in the molten state vigorously attacks glass, ceramics, copper, and graphite. Contaminants significantly influence spectroscopic and structural measurements [12,13] and can strongly distort work function values even in minute presence on the sample surface [14,15]. Since $dW/dT \sim 10^{-4}$ eV/K, precise and contamination-free measurements are necessary to trace out the $W(T)$ curve and resolve the isotopic variations.

We accomplish this by determining the work functions via photoionization of free isolated nanoparticles [16]. Their short flight time within the nanocluster beam apparatus and small surface area ensure the absence of contamination; then a careful measurement of their near-threshold photoionization provides the requisite fraction-of-a-percent precision in assigning the ionization energy over a wide temperature range.

Method.—The apparatus, described in detail in [16], produces metal nanoparticles using a gas aggregation source. A resistively heated stainless-steel crucible is loaded with oxide-free lithium metal, either naturally abundant ^7Li (6.94 standard atomic weight, Sigma-Aldrich) or 95% purity ^6Li (6.02 standard atomic weight, Sigma-Aldrich ISOTEC). The resulting metal vapor is quenched within a continuous flow of ultrahigh purity helium that is cooled by a liquid nitrogen-filled jacket surrounding the aggregation region. Transported by the helium gas, the metal vapor condenses into pure nanoparticles which are then carried through a “thermalization tube” where they are equilibrated to an internal temperature adjustable between 60 K and 360 K, with an accuracy of approximately 1 K [16,17]. Finally, the nanoparticles exit into vacuum as a directed beam.

This beam is populated by a distribution of nanoparticle sizes, which is characterized by time-of-flight mass spectrometry. The distribution is found to be lognormal, as is typical of aggregation/condensation sources [18]. The average size was $\bar{N} \approx 7500$ and 9000 atoms during ^7Li and ^6Li measurements, respectively, and the full-width-at-half-maximum was of the same magnitude, $\Delta N \approx \bar{N}$. Converting this distribution into a distribution of particle radii gives average values of 3.2 and 3.4 nm, respectively. Here $R = r_s a_0 N^{1/3}$, a_0 is the Bohr radius and $r_s = 3.25$ is the Wigner-Seitz electron density parameter of lithium.

After a free flight path of approximately 10 ms duration, the nanoparticle beam is photoionized by a Xe or Hg-Xe arc lamp through a monochromator (UV wavelength calibration accurate to <1 nm, as checked at the beginning of every experiment, and bandwidth <0.4 nm). Because the ionization process is a single-photon one, the detected cation count (normalized to both photon and particle fluxes) is equivalent to the photoelectron yield $Y(h\nu)$, where $h\nu$ is the photon energy. It has been found (see [16] and references therein]) that for nanocluster particles the yield curve closely follows the so-called Fowler formula [19-21] describing photoemission from metal surfaces:

$$\log\left(\frac{Y}{T^2}\right) = B + \log f\left(\frac{h\nu - I}{k_B T}\right) \quad (2)$$

Here I is the ionization energy, B is a temperature-independent coefficient incorporating fundamental constants and instrumental parameters, and f is an integral over a portion of the Fermi-Dirac distribution function (counting those electrons which are moving toward the surface with sufficient energy to transition into the continuum after absorbing a photon).

Since the nanoparticle beam contains a distribution of sizes, and the average of the distribution shifts slightly between measurement runs, it is useful to represent the data in a consistently scaled way. We do this by extrapolating all ionization energies I to the bulk work function limit by means of the scaling relation

$$I(T) = W(T) + \alpha \frac{e^2}{R}, \quad (3)$$

Here R is the particle radius defined above, and the experimental value [22] of the coefficient α for Li is 0.31–0.33 [23].

In an individual measurement at a specific nanoparticle temperature T , I is determined from a fit of the ionization yield curves $Y(h\nu)$ to Eq. (2), and then the work function corresponding to this temperature is calculated by convoluting Eq. (3) with the particle size distribution determined by time-of-flight mass spectrometry during the same measurement [16,25].

Temperature dependence of the work function; the isotope effect.—Fig. 1 shows the experimental results. In the first place, the data reveal that the temperature variation of the ${}^7\text{Li}$ and ${}^6\text{Li}$ work functions are distinct, manifesting a “work function isotope effect.”

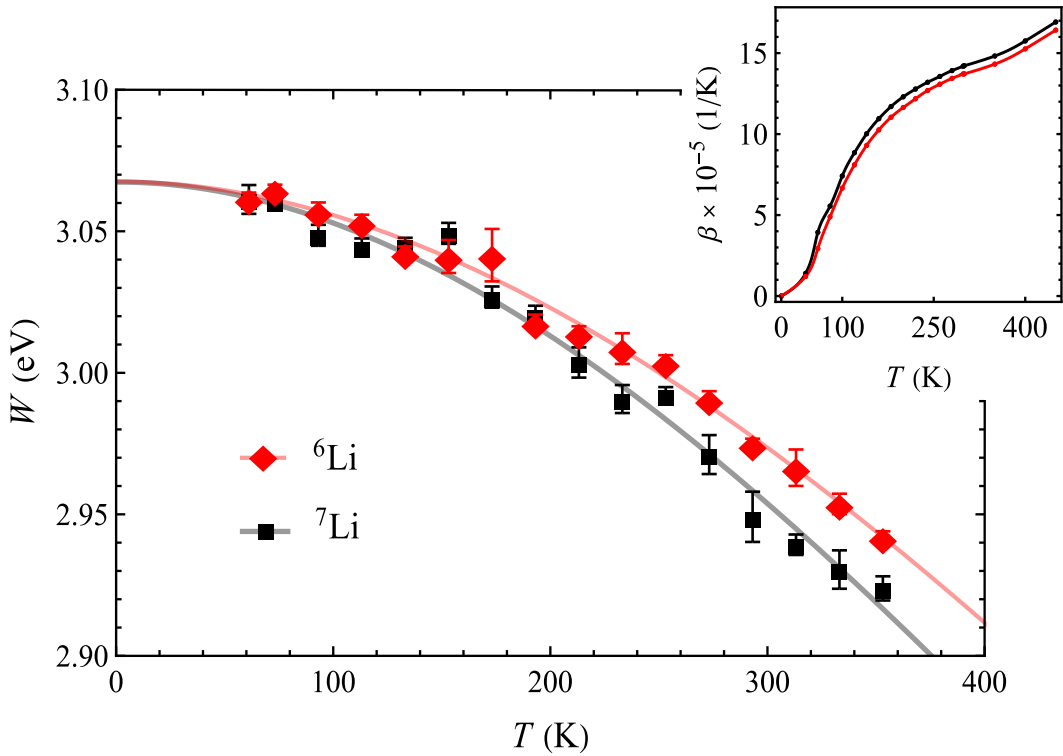


FIG. 1. Experimentally determined work functions of lithium isotopes, ${}^7\text{Li}$ (squares) and ${}^6\text{Li}$ (diamonds). The error bars represent the standard error, typically $\sim 0.3\%$, derived from three individual photoionization measurements at each temperature. (Below 150 K, where the variation of W becomes small, five individual measurements at each temperature were performed.) The solid lines are least-square polynomial fits to the data. The inset shows the volume thermal expansion coefficients of ${}^7\text{Li}$ (black top line) and ${}^6\text{Li}$ (red bottom line) based on data from [28].

Also noteworthy is the fact that the temperature dependence of W here is pronouncedly more nonlinear than for other alkali metals [17,27]. The reason is that the thermal expansion coefficient of Li (see the inset of Fig. 1 [28]) varies with temperature more rapidly than that of the heavier alkalis. This derives from the fact that the Debye temperatures of the latter are significantly smaller, and therefore their heat capacities – and consequently their thermal expansion coefficients, related via the Grüneisen formula – remain relatively unchanged until much lower temperatures [29].

The inset of Fig. 1 also shows that ${}^7\text{Li}$ has a greater thermal expansion coefficient than ${}^6\text{Li}$, which is consistent with the steeper temperature dependence of its work function.

Nonetheless, our measurements indicate that in lithium metal the temperature variation of $W(T)$ entails phenomena beyond only an expansion-related change in the density of the electron gas. The anticipated importance of additional quantum-mechanical effects was already alluded to in the Introduction. The present corroborating experimental evidence derives from a strong mismatch between the Li $W(T)$ data and an electron gas-based image charge model which is successful for free electron-like metals such as Na and K.

In this model the work function is treated as the energy required to remove a charge from a distance d outside the planar surface to infinity, where d is on the order of the screening length in an electron gas and is therefore fully defined by the density of the latter (see the discussion and references in [30,31]). Based on this picture and on the tabulated thermal expansion coefficients, the temperature dependence of the work functions of polycrystalline metals can be evaluated, including accounting for exchange and correlation effects, as described in [32]. As stated above, the results were found to be in good quantitative agreement with data on other alkalis such as Na and K (see, e.g., [17]), signifying that for these metals the electron gas density is indeed the dominant factor.

However, when we repeat the same calculation [32] for Li by using its experimental thermal expansion data (inset of Fig. 1) we find a significant discrepancy: the experimental $W(T)$ curves are much steeper than expected from this treatment. This is clearly seen in Fig. 2. Neither the magnitude of the slopes nor the difference between the isotopes is adequately reproduced by the electron-gas model.

This raises an important challenge for theory: to quantitatively account for the influence of thermal and zero-point atomic vibrations, including the isotope effect, on the electronic work function of lithium. As pointed out already in the classic review [9], there are at least half a dozen effects which can contribute to the dependence of W on temperature. These include, for example, the fact that the effective electrostatic potential experienced by the conduction electrons is altered by the thermal vibrations of the atoms. In a manner of speaking, this may be viewed as an interesting example of *dynamical* electron-phonon coupling modifying a *static* electronic spectral property (the work function).

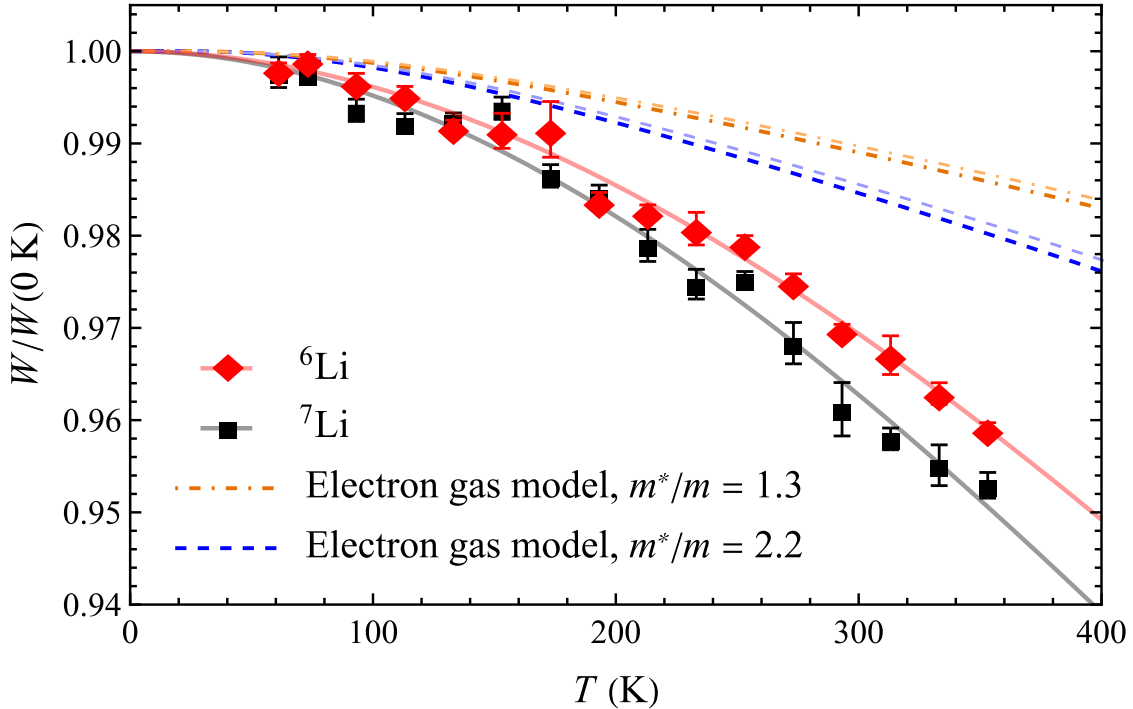


FIG. 2. Fractional shift of the work function with temperature. The data points and solid lines are taken from Fig. 1. The dashed lines follow the formalism of the electron gas model [32], computed using the thermal expansion data from the inset of Fig. 1 (each close-lying pair of lines corresponds to the two lithium isotopes) Since the electron mass enters the calculation as a parameter, the possible influence of the lithium effective mass on the results was explored. The plot shows two options: thermal effective mass $m^* \approx 2.2m$ [8] and band effective mass $m^* \approx 1.3 m$ [33,34]. Neither one can reproduce the curvature of the experimental plot (using the free electron mass m would increase the discrepancy even more), nor the magnitude of the isotope splitting. This attests to the fact that the effect of lattice vibrations on the electronic work function extends beyond only an electron gas density change.

A model endeavoring to approximate this effect by replacing the ionic pseudopotential radius by a thermally diluted value [35] did predict a steeper $W(T)$ dependence for Li, indicating that the ionic potential correction is indeed relevant. However, the same calculation strongly overestimated the thermal shift of W for Na and overestimated it for Al [32], for both of which the electron-gas

image charge model discussed above was quite successful [17,36]. Therefore it is evident that there remains a strong need for a consistent and systematic microscopic treatment.

The low temperature limit of work function.—At low temperatures, the freezing out of the vibrational degree of freedoms decreases the thermal expansion. This translates into a weaker temperature dependence of the work function at low temperature, as observed in Fig 1. The $W(T \rightarrow 0)$ values extrapolated from the experimental curves are the same for both isotopes: $3.068 \text{ eV} \pm 0.003 \text{ eV}$ for ${}^6\text{Li}$ and $3.068 \text{ eV} \pm 0.004 \text{ eV}$ for ${}^7\text{Li}$.

The value recommended in the comprehensive literature review [37] for the work function of polycrystalline ${}^7\text{Li}$ is $2.90 \pm 0.03 \text{ eV}$. Viewed as a room-temperature value, this is in close agreement with the data plotted in Fig. 1, validating the accuracy of the present experiment.

The onset of flattening of the $W(T)$ curves aligns well with the temperature at which the thermal expansion shown in the inset experiences a steep decline, reinforcing the correlation between the electronic work function and the vibrational degrees of freedom.

The actual fact that $dW/dT \rightarrow 0$ as $T \rightarrow 0$ can be established on general grounds, following the argument given in [9]. Starting with Eq. (1), one writes

$$\frac{dW}{dT} = -e \frac{d(\Delta\phi)}{dT} - \frac{d\bar{\mu}}{dT} \quad (4)$$

The first term on the right-hand side is defined by electrostatics, and its variation is caused by thermal expansion. Since the thermal expansion coefficient itself scales with the heat capacity of the material, it must vanish for $T \rightarrow 0$ (this can be seen in the inset in Fig. 1). It follows that $d(\Delta\phi/dT) \rightarrow 0$. As regards the second term, one uses the Maxwell relation

$$\left(\frac{\partial \bar{\mu}}{\partial T} \right)_{P,N} = - \left(\frac{\partial S}{\partial N} \right)_{T,P} \quad (5)$$

Since for $T \rightarrow 0$ entropy approaches a constant (zero), $\partial S/\partial N$ tends to zero and so does the derivative of the chemical potential. Hence in total $dW/dT \rightarrow 0$. Thus, elegantly, the behavior of the work function in Fig. 1 supplies an illustration of the Third Law of Thermodynamics.

Conclusions.—Accurate measurements of the work function of lithium metal, enabled by the use of high purity nanoparticles in a beam, reveal that its temperature dependence exhibits an

isotope effect. The detection of this difference between ^7Li and ^6Li demonstrates that the work function can serve as a probe of the interplay between the electronic and structural degrees of freedom.

The temperature variation of the lithium work function is significantly steeper than predicted by a model that incorporates only thermal expansion of the electron gas, which is sufficient for describing the behavior of metals such as Na and K. This implies that the effect of lattice dynamics on the work function of lithium metal joins the set of other properties of this material that are quantum-mechanical in nature, and is in need of a comprehensive microscopic understanding.

The approach illustrated here can be extended to lower temperatures and to associated systems. For example, bulk ^7Li undergoes a martensitic transition below approximately 77 K, while the behavior of ^6Li is quite different [3]. An isotope-resolved work function measurement taken at small temperature steps and extending to lower nanoparticle temperatures may yield evidence of analogous phenomena at the nanoscale. Another interesting possibility would be to use a dual-oven condensation source to produce beams of metal-fullerene nanoparticles $\text{M}_x(\text{C}_{60})_n$ [38,39], using accurate photoionization measurements to identify the amount of charge transfer and the formation of packing structures in these prototype fulleride compounds.

Acknowledgment

We would like to thank Prof. Shanti Deemyad for a useful discussion. This research was supported by the U.S. National Science Foundation under Grant No. DMR-2003469.

References

1. D. L. Martin, Specific heats of lithium isotopes from 20° to 300°K, *Physica* **25**, 1193 (1959).
2. C. Filippi and D. M. Ceperley, Path-integral Monte Carlo calculation of the kinetic energy of condensed lithium, *Phys. Rev. B* **57**, 252 (1998).
3. G. J. Ackland, M. Dunuwille, M. Martinez-Canales, I. Loa, R. Zhang, S. Sinogeikin, W. Cai, and S. Deemyad, Quantum and isotope effects in lithium metal, *Science* **356**, 1254 (2017).
4. S. Racioppi, I. Saffarian-Deemyad, W. Holle, F. Belli, J. S. Smith, C. Kenney-Benson, R. Ferry, E. Zurek, and S. Deemyad, Lithium's low-temperature phase transitions: Insights into quantum lattice dynamics and superconductivity, *Phys. Rev. B* **111**, 054111 (2025).
5. W. A. Harison, *Pseudopotentials in the Theory of Metals* (Benjamin, New York, 1966).
6. N. W. Ashcroft, Electron-ion pseudopotentials in the alkali metals, *J. Phys. C: Solid State Phys.* **1**, 232 (1968).
7. C. Ellert, M. Schmidt, C. Schmitt, H. Haberland, and C. Guet, Reduced oscillator strength in the lithium atom, clusters, and the bulk, *Phys. Rev. B* **59**, R7841 (1999).
8. C. Kittel, *Introduction to Solid State Physics*, 8th ed. (Wiley, New York, 2005).
9. C. Herring and M. H. Nichols, Thermionic emission, *Rev. Mod. Phys* **21**, 185 (1949).
10. N. D. Lang and W. Kohn, Theory of metal surfaces: Work function, *Phys. Rev. B* **3**, 1215 (1971).
11. *Lithium Chemistry : A Theoretical and Experimental Overview*, ed. by A.-M. Sapse and P. von R. Schleyer (Wiley, New York, 1995).
12. C. C. Addison, *The Chemistry of the Liquid Alkali Metals* (Wiley, New York, 1983).
13. D. W. Jeppson, J. L. Ballif, W. W. Yuan, and B. E. Chou, *Lithium Literature Review: Lithium's Properties and Interactions*, Report HEDL-TME 78-15 (Hanford Engineering Development Laboratory, Richland, 1978).
14. S. Halas and T. Durakiewicz, Is work function a surface or a bulk property?, *Vacuum* **85**, 486 (2010).
15. A. Etxebarria, S. L. Koch, O. Bondarchuk, S. Passerini, G. Teobaldi, and M. Á. Muñoz-Márquez, Work function evolution in Li anode processing. *Adv. Energy Mater.* **10**, 2000520 (2020).
16. A. Sheekhoon, A. Haridy, S. Pedalino, and V. V. Kresin, Photoionization of temperature-controlled nanoparticles in a beam: Accurate and efficient determination of ionization energies and work functions, *Rev. Sci. Instrum.* **96**, 123705 (2025).
17. A. Haridy, A. Sheekhoon, and V. V. Kresin, Temperature-dependent photoionization thresholds of alkali-metal nanoparticles reveal thermal expansion and the melting transition,

Phys. Rev. B **113**, L041404 (2026).

18. H. Haberland, in *Gas-Phase Synthesis of Nanoparticles*, ed. by Y. Huttel (Wiley, Weinheim, 2017).
19. R. H. Fowler, *Statistical Mechanics*, 2nd ed. (Cambridge University Press, Cambridge, 1936).
20. R. H. Fowler, The analysis of photoelectric sensitivity curves for clean metals at various temperatures, Phys. Rev. **38**, 45 (1931).
21. M. Cardona and L. Ley, in *Photoemission in Solids I*, ed. by M. Cardona and L. Ley (Springer, Berlin, 1978).
22. P. Lievens, P. Thoen, S. Bouckaert, W. Bouwen, F. Vanhoutte, H. Weidele, R. E. Silverans, A. Navarro-Vázquez, and P von Ragué Schleyer, Ionization potentials of Li_nO ($2 \leq n \leq 70$) clusters: Experiment and theory, J Chem Phys **110**, 10316 (1999).
23. The variation of r_s with the isotope mass and with temperature may be neglected here: the lattice constant of ${}^6\text{Li}$ exceeds that of ${}^7\text{Li}$ only by a fractional difference of 4×10^{-4} [24], and linear thermal expansion changes the lattice constants only by a fraction of $\approx 10^{-2}$ over the entire investigated temperature range. For the nanoparticle sizes studied here, the resulting correction to W is no more than 2 meV at the limits of the temperature range. This below the precision of the measurement and represents only 1% of the observed shift which is plotted in Fig. 1.
24. E. J. Covington and D. J. Montgomery, Lattice constants of separated lithium isotopes, J. Chem. Phys. **27**, 1030 (1957).
25. The experiment confirmed the extreme sensitivity of the alkali metal's photoelectric threshold to even tiny amounts of surface impurities [26]. Measurements at 180 K and 200 K for ${}^6\text{Li}$ took place in the presence of a minute leak in the source helium supply line. This immediately revealed itself via a ~ 50 meV drop in the experimental work function values. These points were removed from the plotted data.
26. B. B. Alchagirov, L. Kh. Afaunova, F. F. Dyshekova, and R. Kh. Arkhestov, Lithium electron work function: State of the art, Tech. Phys. **60**, 292 (2015).
27. Kh. I. Ibragimov and V. A. Korol'kov, Temperature dependence of the work function of metals and binary alloys, Inorg. Mater. **37**, 677 (2001).
28. T. N. Melnikova and A. G. Mozgovoi, Lithium isotope density and thermal-expansion, High Temp. **26**, 848 (1988).
29. T. N. Mel'nikova and A. G. Mozgovoi, Density, thermal-expansion, and compressibility of sodium and potassium in the solid-phase, High Temp. **27**, 382 (1989).
30. S. Halas and T. Durakiewicz, Work functions of elements expressed in terms of the Fermi

energy and the density of free electrons, *J. Phys.: Condens. Matter* **10**, 10815 (1998).

- 31. T. Durakiewicz, S. Halas, A. Arko, J. J. Joyce, and D. P. Moore, Electronic work-function calculations of polycrystalline metal surfaces revisited, *Phys. Rev. B* **64**, 045101 (2001).
- 32. T. Durakiewicz, A. J. Arko, J. J. Joyce, D. P. Moore, and S. Halas, Thermal work function shifts for polycrystalline metal surfaces, *Surf. Sci.* **478**, 72 (2001).
- 33. K. Yabana and G. F. Bertsch, Ionic core effects on the Mie resonance in lithium clusters, *Z. Phys. D* **32**, 329 (1995).
- 34. S. A. Blundell and C. Guet, Nonlocal ion potential effects on the optical response of lithium clusters, *Z. Phys. D* **33**, 153 (1995).
- 35. A. Kijena, On the temperature dependence of the work function, *Surf. Sci.* **178**, 349 (1986).
- 36. A. Halder and V. V. Kresin, Nanocluster ionization energies and work function of aluminum, and their temperature dependence, *J. Chem. Phys.* **143**, 164313 (2015).
- 37. H. Kawano, Effective work functions of the elements, *Prog. Surf. Sci.* **97**, 100583 (2022).
- 38. T. P. Martin, U. Zimmermann, N. Malinowski, M. Heinebrodt, S. Frank, and F. Tast, Clusters of Fullerene Molecules and Metal Atoms, *Phys. Scripta* **T66**, 38 (1996).
- 39. N. Malinowski, W. Branz, I. M. L. Billas, M. Heinebrodt, F. Tast, and T. P. Martin, Cluster assemblies of metal-coated fullerenes, *Eur. Phys. J. D* **9**, 41 (1999).